Reversible Metal–Metal Bond Cleavage in $FeCo_2$ and FeCoW Clusters

Roy P. Planalp and Heinrich Vahrenkamp*

Institut für Anorganische und Analytische Chemie der Universität, D-7800 Freiburg, Germany

Received July 24, 1986

The clusters (μ_3-MeP)$FeCo_2(CO)_9$ (**1**) and (μ_3-MeP)FeCoWCp'$(CO)_8$ (**2a**, Cp' = C_5H_5, and **2b**, Cp' = C_5Me_5) add 2 mol of the phosphine ligand PMe_3 or PMe_2Ph to form the corresponding clusters (μ_3-MeP)-$FeCo_2(CO)_9(PMe_3)_2$ (**5**) and (μ_3-MeP)FeCoWCp'$(CO)_8(PR_3)_2$ (**3**, Cp' = C_5H_5, and **4**, Cp' = C_5Me_5) in which two metal–metal bonds have been opened. The crystal structure determination of (μ_3-MeP)-$FeCoWC_5H_5(CO)_8(PMe_3)_2$ [**3a**; orthorhombic, $P2_12_12_1$, a = 19.289 (3) Å, b = 11.295 (2) Å, c = 12.881 (3) Å, V = 2806.5 (2) Å^3, Z = 4] reveals PMe_3 addition at iron and cobalt and loss of the Fe–Co and W–Co bonds. Heating the addition compounds in vacuum leads to re-formation of closed clusters: **5** eliminates two CO ligands to form (μ_3-MeP)$FeCo_2(CO)_7(PMe_3)_2$ (**7**); clusters **3** eliminate CO and PR_3 to form (μ_3-MeP)$FeCoWC_5H_5(CO)_7(PR_3)$ (**6**). The phosphine-substituted closed clusters are also the products of thermal phosphine reactions of the starting clusters. A kinetic study has shown the reaction of (μ_3-MeP)-$FeCoWC_5H_5(CO)_8$ (**2a**) with PMe_2Ph in decalin to be first order in complex and first order in phosphine which implies an associative mechanism for the rate-determining step. Optically active **2a** is transformed by PMe_2Ph into optically active (μ_3-MeP)$FeCoWC_5H_5(CO)_8(PMe_2Ph)_2$ (**3b**) that is racemized in solution by a first-order rate law. This allows the interpretation that the racemization of the optically active PFeCoW cluster under CO occurs by an opening–inversion–closing sequence.

Introduction

The formation and reactivity of metal–metal bonds are important aspects of metal cluster reactivity.[1] Basic[1] as well as application-oriented[2] reactions of clusters may originate from metal–metal bond opening and closing. Transition-metal clusters that are "capped" by a main-group moiety such as RP,[3] S,[4] or RC[5] are good candidates for the study of metal–metal bond cleavage and formation since the capping group preserves the integrity of the molecule. But so far mechanistic studies of this type have appeared mainly for binuclear systems,[6] whereas little is known[3,7] involving cluster compounds.

In the course of our investigations of catalysis by mixed-metal clusters[8] we noticed during attempts to perform optical induction by means of optically active clusters that catalytic activity and racemization occurred under similar conditions. A typical observation was that optically active **2a** which is obtained from **1** through metal exchange is racemized under CO pressure.[9] The assumption that metal–metal bond opening is involved in this process was supported by the observation that solutions of **1** and **2a** turn pale under CO pressure, but CO addition products could not be isolated due to re-formation of **1** and **2a** upon workup.[9]

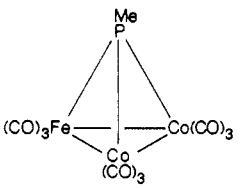

1

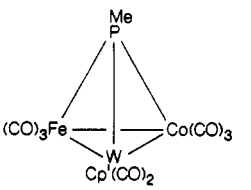

2a, Cp' = C_5H_5
b, Cp' = C_5Me_5

In order to gain some insight into this situation and to possibly draw some general conclusions with respect to cluster opening, we have now investigated the reactions of **1** and **2** type clusters with the more basic and substitution-inert phosphine ligands. This paper describes the isolation of metal–metal bond cleavage products of these clusters and a detailed study of their reactivity and the kinetics and stereochemistry of their formation.

Experimental Section

General Information. All procedures were carried out under an atmosphere of prepurified nitrogen by using standard Schlenk techniques and dry, degassed solvents. Monitoring of reactions by TLC, when possible without decomposition, was effected with aluminum-foil silica gel plates (Merck). Melting points were determined in sealed capillaries. ^1H NMR spectra were determined at 60 MHz (Varian T-60A) by using Me_4Si as internal standard and ^{31}P spectra at 81 MHz (Bruker WP-200) using 85% H_3PO_4 as external standard. All IR measurements, including the quantitative determinations for the kinetic analysis, were performed on a Perkin-Elmer 782 spectrometer in *n*-hexane or decalin solutions.

EI mass spectra were determined with a Finnegan 4000 mass spectrometer at an ionizing energy of 70 eV. Field desorption mass spectra were obtained with a VEGE-700 (Varian). Optical

(1) (a) Vahrenkamp, H. *Angew. Chem.* **1978**, *90*, 403; *Angew. Chem., Int. Ed. Engl.* **1978**, *17*, 379. (b) Chisholm, M. H., Ed. *Reactivity of Metal-Metal Bonds*; ACS Symposium Series 155; American Chemical Society: Washington, DC, 1981. (c) Vahrenkamp, H. *Adv. Organomet. Chem.* **1983**, *22*, 169. (d) Adams, R. D.; Horvath, I. T. *Prog. Inorg. Chem.* **1985**, *33*, 127.

(2) (a) Muetterties, E. L.; Krause, M. J. *Angew. Chem.* **1983**, *95*, 135; *Angew. Chem., Int. Ed. Engl.* **1983**, *22*, 135. (b) Sappa, E.; Tiripicchio, A.; Braunstein, P. *Coord. Chem. Rev.* **1985**, *65*, 219.

(3) (a) Müller, M.; Vahrenkamp, H. *Chem. Ber.* **1983**, *116*, 2311. (b) Schneider, J.; Zsolnai, L.; Huttner, G. *Chem. Ber.* **1982**, *115*, 989.

(4) (a) Richter, F.; Vahrenkamp, H. *Organometallics* **1982**, *1*, 756. (b) Curtis, M. D.; Butler, W. M. *J. Chem. Soc., Chem. Commun.* **1980**, 998. (c) Adams, R. D.; Horvath, I. T.; Kim, H. S. *Organometallics* **1984**, *3*, 548.

(5) (a) Seyferth, D. *Adv. Organomet. Chem.* **1976**, *14*, 98. (b) Beurich, H.; Vahrenkamp, H. *Chem. Ber.* **1982**, *115*, 2385. (c) Jeffery, J. C.; Lawrence-Smith, J. G. *J. Organomet. Chem.* **1985**, *280*, C34.

(6) (a) Langenbach, H. J.; Vahrenkamp, H. *Chem. Ber.* **1979**, *112*, 3390. (b) Jackson, R. A.; Kanluen, R.; Poe, A. J. *Inorg. Chem.* **1981**, *20*, 1130. (c) Jackson, R. A.; Kanluen, R.; Poe, A. J. *Inorg. Chem.* **1984**, *23*, 523. (d) Breen, M. J.; Duttera, M. R.; Geoffroy, G. L.; Novotnak, G. C.; Roberts, D. A.; Shulman, P. M.; Steinmetz, G. R. *Organometallics* **1982**, *1*, 1008. (e) Jones, R. A.; Wright, T. C. *Organometallics* **1983**, *2*, 1842. (f) Mercer, W. C.; Whittle, R. R.; Burkhardt, E. W.; Geoffroy, G. L. *Organometallics* **1985**, *4*, 68. (g) Leonhard, K.; Werner, H. *Angew. Chem.* **1977**, *89*, 656; *Angew. Chem., Int. Ed. Engl.* **1977**, *16*, 649. (h) Roberts, D. A.; Mercer, W. C.; Zahurak, S. M.; Geoffroy, G. L.; DeBrosse, C. W.; Cass, M. E.; Pierpont, C. G. *J. Am. Chem. Soc.* **1982**, *104*, 910.

(7) (a) Schneider, J.; Huttner, G. *Chem. Ber.* **1983**, *116*, 917. (b) Gusbeth, P.; Vahrenkamp, H. *Chem. Ber.* **1985**, *118*, 1758. (c) Knoll, K.; Huttner, G.; Zsolnai, L.; Jibril, I.; Wasiucionek, M. *J. Organomet. Chem.* **1985**, *294*, 91. (d) Schneider, J.; Minelli, M.; Huttner, G. *J. Organomet. Chem.* **1985**, *294*, 75.

(8) Mani, D.; Vahrenkamp, H. *J. Mol. Catal.* **1985**, *29*, 305. Pittman, C. U.; Richmond, M.; Absi-Halabi, M.; Beurich, H.; Richter, F.; Vahrenkamp, H. *Angew. Chem.* **1982**, *94*, 805; *Angew. Chem., Int. Ed. Engl.* **1982**, *21*, 780.

(9) Müller, M.; Vahrenkamp, H. *Chem. Ber.* **1983**, *116*, 2748.

0276-7333/87/2306-0492$01.50/0

Table I. Characterization of New Compounds

compd	color	mp, °C	formula (mol wt)	anal. calcd (found) C	H	Fe
2b	black	145 dec	$C_{19}H_{18}CoFeO_8PW$ (704.95)	32.38 (32.32)	2.56 (2.34)	7.93 (7.10)
3a	dark red	123 dec	$C_{20}H_{26}CoFeO_8P_3W$ (786.97)	30.56 (30.62)	3.33 (3.19)	7.11 (7.41)
3b	red	96	$C_{30}H_{30}CoFeO_8P_3W$ (911.11)	39.59 (39.26)	3.32 (3.30)	6.14 (5.17)
4a[a]	black	180 dec	$C_{25}H_{36}CoFeO_8P_3W$ (857.11)	35.07 (34.56)	4.24 (4.05)	6.52 (5.73)
4b	violet	115	$C_{35}H_{40}CoFeO_8P_3W$ (981.25)	42.89 (42.46)	4.11 (3.79)	5.70 (4.95)
5	dark red	92	$C_{16}H_{21}CoFe_2O_9P_3$ (623.97)	30.77 (31.06)	3.37 (3.13)	8.95 (9.30)
6a	green	152	$C_{16}H_{17}CoFeO_8P_2W$ (698.88)	28.15 (28.35)	2.49 (2.11)	8.19 (7.72)
6c	green	172	$C_{31}H_{23}CoFeO_7P_2W$ (869.10)	42.88 (42.21)	2.65 (2.74)	6.44 (5.88)
6d	green	153	$C_{26}H_{21}CoFeO_7P_2W$ (807.03)	38.75 (38.14)	2.61 (2.92)	6.93 (5.97)
7	green	65	$C_{13}H_{21}Co_2FeO_7P_3$ (555.94)	29.58 (30.13)	3.70 (3.66)	9.84 (9.25)

[a] Oxygen analysis: calcd, 14.95; found, 14.68.

rotation values were measured with a Perkin-Elmer PE-241 polarimeter. The starting materials (-)-(μ_3-MeP)FeCoW(C_5H_5)(CO)$_8$, ((-)-**2a**),[9] (μ_3-MeP)FeCoW(C_5H_5)(CO)$_8$ (**2a**),[8] and (μ_3-MeP)-$FeCo_2$(CO)$_9$ (**1**),[3a] and [W(C_5Me_5)(CO)$_3$]$_2$[10] were synthesized by literature routes. All new compounds are characterized in Table I.

W(C_5Me_5)(CO)$_3$K. A mixture of [W(C_5Me_5)(CO)$_3$]$_2$ (1.5 g, 1.9 mmol) and Na/K alloy (0.4 g) was stirred vigorously in THF (100 mL) for 4 h. The red solution turned pale orange. The solution was filtered and evacuated to dryness, giving a pale yellow powder: yield 1.3 g (79%); IR (THF) 1878 s, 1768 s, 1735 s cm^{-1}.

W(C_5Me_5)(CO)$_3$AsMe$_2$. A solution of W(C_5Me_5)(CO)$_3$K (2.28 g, 5.15 mmol) and $AsMe_2Cl$ (0.46 mL, 4.6 mmol) in cyclohexane (80 mL) and THF (80 mL) was stirred at 0 °C for 1 h, then warmed to room temperature, and stirred for 3 h. The pale orange solution darkened slightly. The solvent was removed at 0–10 °C. The orange-yellow solid was extracted with hexane (2 × 50 mL), filtered, concentrated to ca. 10 mL, and cooled (-30 and then -78 °C). The yellow-brown needles were isolated, and the mother liquor was concentrated to give further product: yield 1.86 g (71%); IR (THF) 1982 s, 1906 s, 1894 vs cm^{-1}; ^{1}H NMR (C_6D_6) 1.47 (s, 6 H), 1.65 (s, 15 H); mp 62 °C. Anal. Calcd for $C_{15}H_{21}AsO_3W$: C, 35.45; H, 4.14. Found: C, 35.96; H, 4.04.

(μ_3-MeP)FeCoW(C_5Me_5)(CO)$_8$ (2b). A solution of W-(C_5Me_5)(CO)$_3$$AsMe_2$ (0.85 g, 1.7 mmol) and **1** (0.79 g, 1.7 mmol) in toluene (75 mL) was stirred for 4 days at 65 °C. A dark red precipitate formed. The solvent was removed under reduced pressure and the solid chromatographed on silica gel by using benzene/hexane (1:2) as eluent. Unreacted **1** (0.15 g, 19%) was recovered in the first fraction, and black-red **2b** (0.37 g, 31%), recrystallized from benzene/hexane, was obtained from the second fraction.

(μ_3-MeP)FeCoW(C_5H_5)(CO)$_8$(PMe_3)$_2$ (3a). Trimethylphosphine (0.071 mL, 0.71 mmol) was added to a dark red solution of **2a** (0.150 g, 0.24 mmol) in benzene (10 mL) at 5 °C. After 45 min, the red solution was slowly diluted with 60 mL of hexane and cooled to -30 °C. Over 2–4 days dark red prisms and needles formed. The crystals were isolated, dried under reduced pressure, and recrystallized once from benzene/hexane; yield 0.083 g (44%) of **3a**.

(μ_3-MeP)FeCoW(C_5H_5)(CO)$_8$(PMe_2Ph)$_2$ (3b). Dimethylphenylphosphine (0.049 mL, 0.34 mmol) was added to a solution of **2a** (0.072 g, 0.11 mmol) in benzene (6 mL). After 1.5 h, the solution was slowly diluted with 60 mL of hexane and crystallized at -30 °C. The wine-red plates were isolated by filtration and dried under reduced pressure; yield 0.077 g (77%) of **3b**. Mass spectrum (EI): m/e 910 (M$^+$), 745 (M$^+$ - PMe_2Ph - CO) for ^{184}W.

(-)-(μ_3-MeP)FeCoW(C_5H_5)(CO)$_8$(PMe_2Ph)$_2$ ((-)-3b). The complex was prepared from (-)-**2a** (0.037 g, 0.58 mmol) and PMe_2Ph (0.017 mL, 0.12 mmol) in benzene (2 mL), adding 15 mL of hexane, following the preparation of **3b** (see above). The yield was 37 mg (71%). Optical rotation [Φ] (heptane, c 0.001 g mL^{-1}): 436 nm, -18 800°; 546 nm, -500°; 578 nm, 4300°. The IR spectrum and the melting point corresponded to those of **3b**.

(μ_3-MeP)FeCoW(C_5Me_5)(CO)$_8$(PMe_3)$_2$ (4a). Trimethylphosphine (0.042 mL) was added to a solution of **2b** (0.10 g, 0.14 mmol) in benzene (10 mL). The dark brown solution turned red over 2 h. The solution was then diluted with 100 mL of hexane and cooled to -30 °C. The black plates were isolated by filtration and dried under reduced pressure; yield 0.10 g (87%) of **4a**. Mass spectrum (FD): m/e 800 (M$^+$ - 2CO), 752 (M$^+$ - PMe_3 - CO) for ^{184}W.

(μ_3-MeP)FeCoW(C_5Me_5)(CO)$_8$(PMe_2Ph)$_2$ (4b). Dimethylphenylphosphine (0.036 mL, 0.26 mmol) was added to a solution of **2b** (0.060 g, 0.085 mmol) in benzene (3 mL). The dark brown solution turned red over 14 h. The solution was diluted with 40 mL of hexane and cooled to -30 °C. The violet needles were isolated by filtration and dried under reduced pressure; yield 0.70 g (84%) of **4b**.

(μ_3-MeP)$FeCo_2$(CO)$_9$(PMe_3)$_2$ (5). A solution of **1** (0.158 g, 0.33 mmol) in benzene (10 mL) was treated with PMe_3 (0.084 mL, 0.84 mmol) and allowed to react until examination of the solution by TLC showed no starting material remaining (1 h). Hexane (50 mL) was added, and the solution was cooled to -30 °C. The black needles were crystallized once from a benzene/hexane mixture; yield 0.124 g (60%) of **5**.

(μ_3-MeP)FeCoW(C_5H_5)(CO)$_7$(PMe_3) (6a). A solution of **3a** (0.085 g, 0.11 mmol) in toluene (10 mL) was refluxed at 60 °C under partial vacuum for 14 h, giving a green solution. The solvent was filtered through silica gel and evaporated to dryness. The dark green solid was crystallized from hexane; yield 0.054 g (74%) of **6a**.

(μ_3-MeP)FeCoW(C_5H_5)(CO)$_7$(PMe_2Ph) (6b), which was already known,[9] was obtained the same way from **3b**.

(μ_3-MeP)FeCoW(C_5H_5)(CO)$_7$(PPh_3) (6c). A solution of **2a** (0.067 g, 0.111 mmol) and PPh_3 (0.138 g, 0.53 mmol) in benzene (10 mL) was heated to 60 °C for 5 h, causing it to turn dark green. The reaction was monitored by TLC. When all starting materials had been converted, the solvent was removed under reduced pressure and the residue crystallized from a hexane/toluene mixture (5:1); yield 0.073 g (79%) of **6c**.

(μ_3-MeP)FeCoW(C_5H_5)(CO)$_7$($PMePh_2$) (6d). A solution of **2a** (0.117 g, 0.185 mmol) and $PMePh_2$ (0.092 mL, 0.554 mmol) in benzene (10 mL) was let stand 12 h. Addition of hexane (40 mL) to the green solution and cooling to -30 °C gave 0.124 g (83%) of dark green prisms of **6d**.

(μ_3-MeP)$FeCo_2$(CO)$_7$(PMe_3)$_2$ (7). A solution of **5** (0.135 g, 0.216 mmol) in toluene (15 mL) was refluxed at 80 °C under partial vacuum for 12 h, giving a green solution. The solution was filtered through silica gel and evaporated to dryness. The green solid was crystallized from benzene/hexane; yield 0.109 g (89%) of **7**.

CO Reactions of 6a and 6b. Solutions of ca. 5 mg of **6a** and **6b** in ca. 10 mL of benzene were treated for 18 h at 60 °C under 65 bar of CO. Immediately after the reaction IR spectra showed that all **6** had been used up. The solutions had turned brownish, and yellow bands could be seen on TLC plates. Evaporation of the solvent left brown oily residues that turned darker upon standing. After prolonged standing, compounds **2a** as well as **6a,b** could be identified in the IR spectra, but among several other unidentified products.

Conversion 7 → 5. A dark green solution of **7** (0.121 g, 0.213 mmol) in hexane (15 mL) was heated for 18 h at 60 °C under 65 bar of CO. The cloudy red solution was filtered and the residue washed with benzene (10 mL). The washings and filtrate were combined, and the dark red solution was diluted with 40 mL of hexane. Cooling to -30 °C gave crystalline **5**, yield 0.12 g (90%).

(10) King, R. B.; Iqbal, M. Z.; King, A. D. *J. Organomet. Chem.* **1979**, *171*, 53.

Table II. Rate Constants for the Reaction (μ_3-MeP)FeCoW(C_5H_5)(CO)$_8$ + 2PMe$_2$Ph in Decalin under Pseudo-First-Order Conditions

10^{-2}[PMe$_2$Ph]$_0$, M	[PMe$_2$Ph]$_0$/ **2a**	T, °C	$10^{-3}K_{obsd}$, s^{-1}	K, M^{-1} s^{-1}
9.14	75	16.0	1.51	0.0165
14.0	100	16.0	2.28	0.0163
20.0	174	16.0	3.42	0.0171
9.14	60	22.0	2.41	0.0263
14.0	100	22.0	3.46	0.0247
14.0	100	22.0	3.83	0.0273
14.0	100	22.0	3.76	0.0269
9.14	60	28.0	3.30	0.0361
9.14	60	28.0	3.29	0.0360
11.7	80	28.0	4.18	0.0357
6.37	40	34.6	3.92	0.0615
6.37	40	34.6	3.82	0.0600
9.14	60	34.6	4.92	0.0538
11.7	80	34.6	6.53	0.0558
6.37	44	37.7	4.18	0.0657
6.37	44	37.7	4.36	0.0684

PR$_3$ Reactions of 3, 4, and 6. Solutions of ca. 10 mg of **3a**, **3b**, **4a**, **4b**, **6a**, and **6b** in ca. 20 mL of benzene were treated with excess PMe$_3$ or PMe$_2$Ph. No reaction occurred at room temperature. At 80 °C, any reaction, if noticeable, was slower than conversions (to **6**) or decomposition.

Kinetic Studies of Bond Cleavage. All kinetic measurements were obtained by direct observance of the reaction progress in thermostated NaCl IR cells (RIIC Ltd.). The temperature of the cells was set by heat exchange with a recirculating bath (Lauda K4R) and monitored by using a Cu–constatan thermocouple in good thermal contact with the cell plates. Temperatures of 10–50 °C were readily accessible with the apparatus.

The overall order of the reaction was first examined by the method of initial rates.[11a] The concentration of metal complex was varied by a factor of 6 and that of phosphine by a factor of 100, employing decalin or tetralin as solvent. The disappearance of IR bands of the starting material **2a** as well as the growth of product bands of **3b** was monitored. By IR monitoring it was also ensured that no more than traces of **6b**, the successor complex of **3b**, were formed. Concentrations c were determined from the relationship $c \propto \log (T_0/T)$, where T_0 is the base-line transmission and T the observed transmission.[11b]

In decalin the reaction orders of 1 in **2a** and 1 in phosphine were determined. In tetralin, comparison of the rate of disappearance of starting material vs. the rate of appearance of product revealed that greater than 40% of the starting material converted to products other than **3b**, reducing the yield by 30% when a fivefold excess of phosphine was employed, and further experiments in this solvent were abandoned. The reaction was studied under pseudo-first-order conditions ([PR$_3$] > 20[**2a**]). The temperatures and concentrations were varied (Table II), and for each run a plot of ln (1/[**2a**]) vs. time was made, to which the parameters k_{obsd} and ln (1/[A]$_0$) were fitted by a least-squares procedure, according to the equation ln (1/[A]) = $k_{obsd}t$ + ln (1/[A]$_0$), for a process first order in A. The reaction was followed for at least 3 half-lives, for which values of k and ln (1/[A]$_0$) were obtained by line fitting with typical standard deviations of 1–2%. The values of k for each temperature were averaged, giving the rate constants listed in Table VIII. Activation energies were calculated from these values on the basis of activated complex theory,[11c] with transformation of the standard derivations to statistical weights.[11d] Table II summarizes the kinetic measurements.

Racemization of (–)-3b. The optical rotations of three heptane solutions of (–)-**3b** (0.001–0.003 M) at 35 °C were measured as a function of time at the wavelengths 436 and 578 nm. Over a period of 3 h, the optical rotation decreased to nearly zero. The final solutions had concentrations of **3b** equal to greater than 90% of the starting concentration, as determined by IR spectroscopy. The rate of decrease in optical activity, taken as the rate of racemization of (–)-**3b**, was independent of the concentration of (–)-**3b** and was evaluated by plots of ln (1/[Φ]) vs. time to give a first-order rate of racemization of 2.5 (4) × 10^{-4} s^{-1}.

Table III. Crystallographic Data for 3a

formula	$C_{20}H_{26}CoFeO_8P_3W$
mol wt	786.97
space group	$P2_12_12_1$
a, Å	19.2889 (30)
b, Å	11.2954 (15)
c, Å	12.8813 (25)
V, Å^3	2806.5 (15)
Z	4
d_{calcd}, g cm^{-3}	1.86
d_{obsd}, g cm^{-3}	1.84
radiation	Ag Kα, 0.560 83 Å
monochromator	graphite
abs coeff (μ), cm^{-1}	27.4
cryst form and size, mm	needle, 0.29 × 0.08 × 0.13
indices measd	$\pm h,+k,+l$
intensity stds	(2, 0, 0); (0, 0, 2)
decay of stds	none
unique data	4820
data, $I \geq 2.5\sigma(I)$	2971
no. of variables	307
scan range, type	2° < 2θ < 42°, ω–2θ
scan speed, deg min^{-1}	0.69–6.7
scan width, deg	0.80 + 0.45 tan θ
T, K	295 ± 1

X-ray Structure Determination. A crystal of complex **3a**, obtained by slow cooling of a benzene/hexane solution from 20 to 0 °C, was mounted on a glass fiber. The crystal was examined by Weissenberg photographs, yielding *mmm* diffraction symmetry and approximate cell dimensions. The crystal was mounted on an Enraf-nonius CAD4 diffractometer controlled by a PDP 8/i computer. The same cell was found, and the systematic absences observed were consistent only with space group $P2_12_12_1$. The final cell parameters were determined from the setting angles of 24 centered reflections (2θ > 25°) from diverse regions of reciprocal space.

The 6716 raw intensity data were reduced to structure factor amplitudes and their esd's by correction from scan speed, background, Lorentz, and polarization effects. An absorption correction was applied. The transmission factor, based on the observed crystal faces and measurements, with a Gaussian grid approximation, varied from 0.8280 to 0.7217.

Systematically absent and redundant reflections were rejected, and a Patterson map was calculated. The position of the tungsten atom was determined, and the complete solution followed by use of Fourier and least-squares techniques. A weighting function was applied (w = 0.7245/($\sigma^2(F)$ + 0.000 15F^2), and a test for the correct enantiomorph was made.[12] In the final full-matrix least-squares cycles, the largest (parameter shift)/esd value was 0.019, with residuals[13] R = 5.32% and R_w = 4.69%. The highest peak in the final difference Fourier map, of density 1.8 e/Å^3, was located 1.03 Å from the tungsten atom. There was no evidence of extinction from the low-angle, high-intensity data. Structure factors were taken from Cromer et al. with corrections for anomalous dispersion,[14] and calculations were performed by using the SHELX76[15] series of programs and drawings with the SCHAKAL84[16] programs. Table III summarizes the crystallographic data, and Table IV gives the atomic parameters.

Results and Discussion

Reactions. In order to facilitate opening of the PM$_3$ clusters by addition of donor ligands, two measures seemed

(11) (a) Laidler, K. J. *Chemical Kinetics*; McGraw-Hill: New York, 1948. (b) Weitkamp, H.; Barth, R. *Einführung in die quantitative Infrarot-Spektrophotometrie*; Georg Thieme Verlag: Stuttgard, 1976. (c) Glasstone, S.; Laidler, K. J.; Eyring, H. *The Theory of Rate Processes*; McGraw-Hill: New York, 1941. (d) Cvetanovic, R. J.; Singleton, D. L. *Int. J. Chem. Kinet.* **1977**, *9*, 481.

(12) Hamilton, W. C. *Acta Crystallogr.* **1965**, *18*, 502.

(13) $R = \sum(||F_o| - |F_c||)/|F_o|$. $R_w = \sum w(||F_o| - |F_c||)/w|F_o|$.

(14) (a) Cromer, D. T.; Mann, L. J. *Acta Crystallogr., Sect. A: Cryst. Phys. Diffr. Theor. Gen. Crystallogr.* **1968**, *A24*, 321. (b) Cromer, D. T.; Bermen, D. J. *J. Chem. Phys.* **1970**, *53*, 1891.

(15) Sheldrick, G. M. University of Leeds, 1976.

(16) Keller, E. Universität Freiburg, 1984.

Table IV. Atomic Parameters for (μ_3-MeP)FeCoW(C_5H_5)$(CO)_8(PMe_3)_2$ (3a)

atom	x	y	z	$U(11)$	$U(22)$	$U(33)$	$U(12)$	U_{13}	$U(23)$	U_{eq}
W	0.1283 (1)	0.1799 (1)	0.2958 (1)	0.0419 (3)	0.0422 (4)	0.0391 (3)	−0.0006 (5)	−0.0006 (4)	0.0004 (5)	0.0419 (3)
Co	0.3406 (1)	0.1028 (3)	0.2556 (2)	0.055 (2)	0.063 (2)	0.057 (2)	0.010 (1)	−0.006 (1)	−0.006 (1)	0.055 (2)
Fe	0.2122 (1)	0.3862 (3)	0.2310 (2)	0.046 (2)	0.045 (2)	0.051 (2)	−0.001 (1)	−0.001 (1)	0.001 (1)	0.046 (2)
P1	0.2370 (2)	0.1928 (5)	0.2040 (4)	0.047 (2)	0.056 (3)	0.041 (2)	0.004 (3)	−0.005 (2)	−0.001 (4)	0.047 (2)
C1	0.2349 (8)	0.152 (2)	0.064 (1)	0.05 (1)	0.07 (2)	0.04 (1)	0.02 (1)	−0.008 (8)	−0.03 (1)	0.05 (1)
P2	0.4364 (3)	−0.0002 (5)	0.2889 (5)	0.071 (4)	0.089 (4)	0.069 (4)	0.020 (3)	−0.007 (4)	−0.010 (4)	0.071 (4)
C21	0.495 (1)	0.065 (3)	0.381 (2)	0.14 (2)	0.25 (4)	0.10 (2)	0.06 (2)	−0.03 (1)	−0.03 (2)	0.14 (2)
C22	0.489 (1)	−0.036 (3)	0.182 (2)	0.17 (3)	0.30 (4)	0.05 (1)	0.16 (3)	−0.01 (2)	−0.03 (2)	0.17 (3)
C23	0.423 (1)	−0.148 (3)	0.347 (3)	0.23 (4)	0.12 (3)	0.46 (7)	0.05 (2)	0.05 (3)	0.17 (4)	0.23 (4)
P3	0.1567 (3)	0.5514 (4)	0.2778 (4)	0.056 (3)	0.043 (3)	0.056 (3)	0.005 (3)	−0.006 (3)	0.005 (3)	0.056 (3)
C31	0.207 (1)	0.652 (2)	0.360 (2)	0.10 (2)	0.04 (2)	0.15 (2)	0.01 (1)	−0.03 (2)	−0.02 (1)	0.10 (2)
C32	0.131 (1)	0.652 (2)	0.175 (1)	0.10 (2)	0.12 (2)	0.08 (1)	0.04 (2)	0.00 (1)	−0.02 (1)	0.10 (2)
C33	0.0783 (9)	0.540 (2)	0.356 (2)	0.08 (2)	0.09 (2)	0.12 (2)	0.02 (1)	0.01 (1)	−0.01 (2)	0.08 (2)
C41	0.056 (1)	0.186 (3)	0.441 (1)	0.08 (2)	0.12 (2)	0.03 (1)	0.00 (2)	0.011 (9)	0.03 (2)	0.08 (2)
C42	0.065 (1)	0.065 (2)	0.412 (2)	0.08 (2)	0.09 (2)	0.05 (1)	−0.02 (2)	0.02 (1)	0.02 (1)	0.08 (2)
C43	0.133 (2)	0.042 (2)	0.422 (1)	0.09 (2)	0.08 (2)	0.05 (1)	−0.02 (2)	0.02 (2)	0.03 (1)	0.09 (2)
C44	0.173 (1)	0.140 (2)	0.465 (2)	0.09 (2)	0.08 (2)	0.04 (1)	0.00 (2)	−0.01 (1)	0.03 (1)	0.09 (2)
C45	0.123 (1)	0.226 (2)	0.477 (1)	0.08 (1)	0.11 (2)	0.023 (9)	−0.01 (2)	0.00 (1)	0.01 (1)	0.08 (1)
C2	0.295 (1)	−0.028 (2)	0.233 (2)	0.07 (2)	0.07 (2)	0.06 (1)	0.02 (1)	0.00 (1)	0.01 (1)	0.07 (2)
O2	0.2660 (9)	−0.115 (1)	0.222 (2)	0.12 (2)	0.06 (1)	0.17 (2)	−0.03 (1)	0.01 (1)	−0.02 (1)	0.12 (2)
C3	0.380 (1)	0.181 (3)	0.158 (2)	0.09 (2)	0.11 (2)	0.13 (2)	0.00 (2)	−0.01 (1)	−0.02 (2)	0.09 (2)
O3	0.4081 (9)	0.236 (2)	0.093 (1)	0.13 (2)	0.18 (2)	0.13 (2)	−0.02 (1)	0.02 (1)	0.02 (1)	0.13 (2)
C4	0.346 (1)	0.164 (3)	0.379 (2)	0.12 (2)	0.18 (3)	0.09 (2)	0.06 (2)	−0.06 (1)	0.00 (2)	0.12 (2)
O4	0.352 (1)	0.200 (2)	0.462 (1)	0.21 (2)	0.29 (3)	0.12 (1)	0.16 (2)	−0.11 (2)	−0.10 (2)	0.21 (2)
C5	0.287 (1)	0.447 (2)	0.184 (2)	0.08 (2)	0.10 (2)	0.06 (2)	0.02 (2)	−0.02 (1)	−0.02 (1)	0.08 (2)
O5	0.3376 (8)	0.487 (2)	0.151 (1)	0.12 (2)	0.18 (2)	0.14 (2)	−0.05 (1)	0.01 (1)	0.02 (1)	0.12 (2)
C6	0.163 (1)	0.388 (2)	0.113 (2)	0.07 (1)	0.04 (1)	0.06 (1)	0.01 (1)	0.01 (1)	0.02 (1)	0.07 (1)
O6	0.1354 (8)	0.394 (1)	0.035 (1)	0.09 (1)	0.12 (1)	0.053 (8)	0.01 (1)	−0.016 (9)	0.033 (9)	0.09 (1)
C7	0.237 (1)	0.381 (2)	0.365 (2)	0.06 (1)	0.03 (1)	0.07 (2)	0.00 (1)	−0.02 (1)	−0.01 (1)	0.06 (1)
O7	0.2547 (8)	0.387 (1)	0.449 (1)	0.08 (1)	0.08 (1)	0.043 (8)	0.007 (9)	−0.022 (8)	−0.001 (8)	0.08 (1)
C8	0.0606 (9)	0.264 (2)	0.212 (2)	0.06 (1)	0.07 (1)	0.06 (1)	−0.02 (1)	0.02 (1)	−0.01 (1)	0.06 (1)
O8	0.0140 (7)	0.307 (1)	0.169 (1)	0.09 (1)	0.08 (1)	0.14 (1)	−0.002 (9)	−0.041 (9)	0.04 (1)	0.09 (1)
C9	0.112 (1)	0.068 (2)	0.202 (4)	0.16 (3)	0.04 (1)	0.39 (5)	0.00 (1)	0.06 (3)	0.08 (3)	0.16 (3)
O9	0.1006 (9)	−0.006 (1)	0.132 (1)	0.10 (1)	0.07 (1)	0.14 (1)	−0.03 (1)	0.00 (1)	−0.02 (1)	0.10 (1)

Table V. IR and ^1H NMR Spectra of New Compounds

		NMR	
no.	IR (hexane) ν(CO), cm^{-1}	solv	shift, ppm (mult, area, J (Hz), assignmt)
2b	2052 s, 2010 vs, 1985 sh, 1977 s, 1964 m, 1956 sh, 1941 m, 1921 m, 1851 w (br)	C_6D_6	2.28 (d, 3, J = 13.8, *Me*P) 1.80 (s, 15, C_5Me_5)
3a	2050 m, 2020 m, 1996 s, 1976 s, 1956 s, 1916 m, 1886 m (br), 1811 m (br)	C_6D_6	5.27 (s, 5, C_5H_5) 2.82 (d, 3, J = 6.6, *me*P) 1.32 (d, 9, J = 9.0) 0.87 (d, 9, J = 9.6) PMe_3
3b	2032 m, 2018 m, 1996 m, 1980 vs, 1958 vs, 1944 m, 1915 m (br), 1894 s, 1826 s, 1822 sh	C_6D_6	7.21 (br, 10, *Ph*Me_2) 5.20 (s, 5, C_5H_5) 2.68 (d, 3, J = 7.2, *Me*P) 1.52 (d, 6, J = 9.0) 1.08 (d, 6, J = 9.6) PMe_2
4a	2037 m, 1991 sh, 1977 vs, 1948 vs, 1913 m (br), 1881 m (br), 1820 m	C_6D_6	2.81 (br d, 3, J = 10.0, *Me*P) 2.22 (s, 15, C_5Me_5) 1.47 (d, 9, J = 9.0) 0.96 (d, 9, J = 10.9) PMe_3
4b	2036 m, 2012 m, 1978 vs, 1952 s, 1921 m (br), 1882 m (br), 1818 m (br)	C_6D_6	7.02 (m, 10, *Ph*PMe_2) 2.60 (d, 3, J = 9.0, *Me*P) 2.15 (s, 15, C_5Me_5) 1.82 (d, 6, J = 8.4) 1.29 (d, 6, J = 9.6) PMe_2
5	2060 w, 2020 m, 1984 vs, 1967 m, 1950 s, 1930 sh	C_6D_6	2.66 (d, 3, J = 14.0, *Me*P) 1.22 (d, 9, J = 9.0) 0.74 (d, 9, J = 10.2) PMe_3
6a	2020 m, 1975 s, 1961 vs, 1940 m, 1920 m, 1914 sh, 1898 m	C_6D_6	4.81 (s, 5, C_5H_5) 2.71 (d, 3, J = 13.2 *Me*P) 1.04 (d, 9, J = 8.4, PMe_3)
6c	2020 m, 1978 m, 1960 vs, 1951 sh, 1940 sh, 1928 w (sh), 1900 w	$CDCl_3$	7.37 (br d, 15, Ph_3P) 5.34 (s, 5, C_5H_5) 2.24 (d, 3, J = 12.6, *Me*P)
6d	2036 sh, 2016 sh, 1971 sh, 1958 vs, 1940 w, 1918 w, 1900	$CDCl_3$	7.38 (br, 10, Ph_2P) 5.29 (s, 5, C_5H_5) 2.36 (d, 3, J = 13.6, *Me*P) 1.89 (d, 3, J = 9.7, *Me*PPh_2)
7	2036 s, 1985 vs, 1972 m, 1965 sh, 1958 sh, 1933 m, 1919 sh, 1912 m	$CDCl_3$	2.72 (d, 3, J = 13.7, *Me*P) 1.32 (d, 18, J = 8.8, PMe_3)

appropriate: increasing the steric bulk in the ligand sphere and using more basic reagents. The latter was realized by taking alkylphosphine donors. The former induced us to synthesize the cluster **2b**, the C_5Me_5 equivalent of **2a**. The route to **2b** was the standard metal exchange sequence[17] starting from **1** with the reagent $C_5Me_5(CO)_3W$–$AsMe_2$ which in turn was obtained from $KW(CO)_3C_5Me_5$ and $AsMe_2Cl$. While the reaction conditions were optimized for cluster opening, it was then found that by running the reactions carefully all three starting clusters (**1**, **2a**, **2b**) are opened by alkylphosphines with comparable ease, the main observation being that under mild conditions addition of donor ligands prevails while under more forcing conditions CO substitution occurs. As discussed by Poë for $Ru_3(CO)_{12}$[18] this opening–closing sequence may well be a general

(17) Vahrenkamp, H. *Comments Inorg. Chem.* **1985**, *4*, 253.

phenomenon for ligand substitutions on clusters.

Both clusters **2a** and **2b** added 2 mol of PMe_3 and PMe_2Ph. The course of the reactions could be followed by the colors of the solutions becoming less intense. **2b** reacted slower than **2a**. The addition products **3a,b** and **4a,b** were isolated in good yields by low-temperature crystallization; they could not be chromatographed and they were labile at room temperature in solution. Accordingly, 1 and PMe_3 formed **5**. With use of optically active **2a**, the reaction with PMe_2Ph produced optically active **3b**, indicating that while the rigidity of the cluster framework is lost, this does not lead to immediate racemization. Over a period of a few hours in solution, however, the optical activity of **3b** disappears (see below).

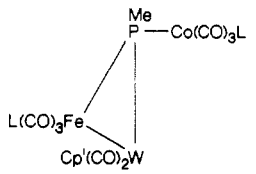

3a, $Cp' = C_5H_5$, $L = PMe_3$
b, $Cp' = C_5H_5$, $L = PMe_2Ph$
4a, $Cp' = C_5Me_5$, $L = PMe_3$
b, $Cp' = C_5Me_5$, $L = PMe_2Ph$

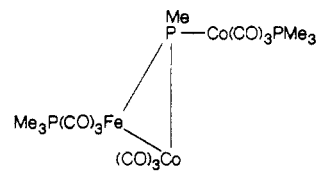

5

With the less basic and more bulky phosphine ligands PPh_3 and PPh_2Me addition products like **3** could not be isolated pure. Following the reactions by TLC indicated that yellow or brownish intermediates were formed which are likely to be the addition products, but only the substitution products **6c** and **6d** were isolated. Analogous reaction sequences could be realized by leaving **3a** and **3b** in solution for longer periods of time, or better by heating their solutions in vacuum. The formation of the resulting compounds **6a** and **6b**, of which **6b** had been obtained before by direct substitution from **2a**,[9] involves loss of CO and phosphine from **3**. Similar observations had been made before for $GeCo_3$ clusters,[7b] and analogous but less clean reactions occurred for **4a** and **4b**. In contrast to this, thermolysis of **5** yielded **7** by loss of CO only. Thus the electron density in the clusters determines whether CO or PR_3 are eliminated preferentially, with the product clusters containing two donor ligands (Cp or PR_3) each. And although the net ligand substitutions from **1** to **7** and from **2** to **6** have different stoichiometries, they are mechanistically equivalent. The change from an open polynuclear framework to a trimetal cluster could again be followed visually with the colors of the clusters being much more intense.

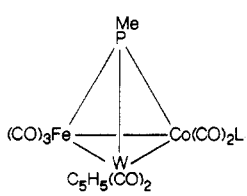

6a, $L = PMe_3$
b, $L = PMe_2Ph$
c, $L = PPh_3$
d, $L = PPh_2Me$

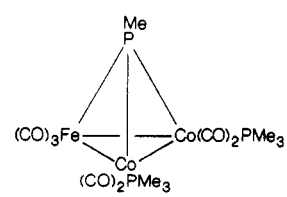

7

In order to find out how far the opening–closing sequences could be extended, some further reactions of compounds **3–7** with donor ligands were performed. There was just one successful attempt with CO: **7** was reconverted to **5** at 60 °C under 65 bar of CO. **6a** and **6b**, however, under CO pressure produced yellow/brownish oils again which could not be obtained pure and which under normal conditions were partly converted back to **6a,b**. This corresponds to the behavior of **1** and **2a**.[9] In contrast, cluster **6** with $L = Ph_2P$–Omenthyl loses this less basic ligand under CO pressure and goes back to **2a** as applied in the enantiomer separation of **2a**.[9]

Attempts to introduce more phosphine ligands (PMe_3 or PMe_2Ph) were unsuccessful for **3a,b**, **4a,b**, and **6a,b**. Except for decomposition of **3** and **4** no reaction occurred up to 80 °C in benzene. This is understandable for **3** and **4** which are labile and where the maximum number of metal–metal bonds seems to be opened. There is no simple explanation, however, for the reluctance of the clusters **6** to go back to clusters similar to **3**, especially when contrasted to the behavior of analogous dinuclear AsM_2 systems into which up to four phosphine ligands could be introduced by such opening–closing sequences.[19]

Constitution of the Products. Tables V and VI list the IR and NMR data of the new complexes. While the IR spectra give no significant structural information, it was obvious from the mass spectrum of **3b** and from the NMR spectra that 2 equiv of phosphine ligand had been added in the products **3–5**. Since one donor ligand added corresponds to one metal–metal bond lost, the general constitution of the addition products was clear. The detailed constitution, i.e. the points of attachment of the phosphine ligands, could be assigned by common sense and by inspection of the NMR data. Common sense expects that one donor ligand (Cp or PR_3) per metal atom is the most likely situation when three donor ligands are present and that the metal–metal bonds involving cobalt are broken first since $Co(CO)_3$ is the best leaving group in cluster framework reactions.[17] This together with the NMR information that there are two nonequivalent PR_3 ligands leads to the given structures for **3** and **4**. But since even the X-ray analysis of **3a** (see below) cannot distinguish iron and cobalt, it must be stated that these assignments are not unambiguous. This most also be said for **5** where according to NMR two nonequivalent PMe_3 groups are present of which due to the line widths in the ^{31}P NMR spectrum only one is bound to cobalt. The constitutions of the clusters **6** could be deduced from the IR spectra with reference to the known **6b**.[9] The ^1H and ^{31}P NMR spectra are in accord with this. A consistent NMR interpretation requires that in the **5** → **7** interconversion one PMe_3 group has moved from iron to cobalt since both ^1H and ^{31}P NMR

Table VI. ^{31}P NMR Data for Selected Compounds

no.	solv	T, K	shift, ppm (mult, area, J (Hz))	assignmt
5	PhMe-d_8	308	188.2 (t, 1, J = 58.0[a]),	μ_3-P
			19.3 (d, 1, J = 55.0),	P^1-Fe
			12.3 (s, 1, $\nu_{1/2}$ = 106 Hz)	P^2-Co
5	PhMe-d_8	243	186.3 (dd, 1, J_{P-P^1} = J_{P-P^2} = 61.0),	μ_3-P
			20.9 (d, 1, J = 55.0),	P^1-Fe
			13.66 (d, 1, J = 69.0)	P^2-Co
6a	CD_2Cl_2	308	361.7 (s, 1, $\nu_{1/2}$ = 580 Hz),	μ_3-P
			11.6 (s, 1, $\nu_{1/2}$ = 680 Hz)	P-Co
7	PhMe-d_8	308	400.1 (s, 1, $\nu_{1/2}$ = 454 Hz),	μ_3-P
			2.9 (s, 2, $\nu_{1/2}$ = 410 Hz)	P-Co
	PhMe-d_8	243	402.6 (s, 1, $\nu_{1/2}$ = 96 Hz),	μ_3-P
			3.8 (s, 2, $\nu_{1/2}$ = 85 Hz)	P-Co

[a] Two overlapping doublets that are resolved in the low-temperature spectrum.

(18) Brodie, N.; Poe, A.; Sekhar, V. *J. Chem. Soc., Chem. Commun.* **1985**, 1090.

(19) Langenbach, H. J.; Vahrenkamp, H. *Chem. Ber.* **1979**, *112*, 3390, 3773.

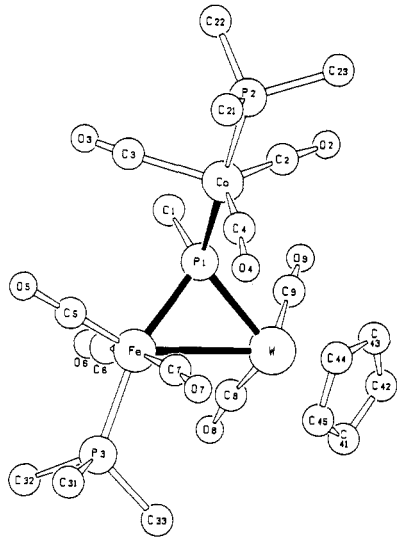

Figure 1. Molecular structure of $(\mu_3\text{-MeP})FeCoWC_5H_5(CO)_8(PMe_3)_2$ (**3a**).

Table VII. Selected Bond Distances (Å) and Angles (deg) in $(\mu_3\text{-MeP})FeCoW(C_5H_5)(CO)_8(PMe_3)_2$ (3a)

	Bond Distances		
Fe–W	2.956 (3)	C2–Co	1.743 (23)
P1–W	2.410 (4)	C3–Co	1.720 (25)
P1–Fe	2.263 (6)	C4–Co	1.730 (26)
P1–Co	2.340 (5)	C5–Fe	1.710 (23)
P2–Co	2.225 (6)	C6–Fe	1.791 (21)
P3–Fe	2.234 (5)	C7–Fe	1.792 (22)
C1–P1	1.861 (17)	C8–W	1.943 (19)
$C(C_5H_5)$–W	2.34 (av)	C9–W	1.767 (35)
	Bond Angles		
W–P1–Fe	78.4 (2)	P1–Co–P2	172.6 (2)
P1–Fe–P3	161.6 (2)	C1–P1–Co	100.7 (5)
Fe–P1–Co	123.8 (2)	C1–P1–Fe	112.5 (6)
W–P1–Co	125.2 (2)	C1–P1–W	116.2 (5)

indicate equivalent PMe_3 groups in **7**. The large line widths due to the quadrupole moment of spin $^7/_2$ ^{59}CO which, as expected, decrease at lower temperatures for **5** and **7** support the assignments of cobalt-bound phosphorus units in clusters **5**, **6**, and **7**.

The NMR data of the compounds **1**–**7** show the typical chemical shift phenomena associated with metal–metal bond making and breaking which are of high diagnostic value, especially using ^{31}P NMR.[20] As observed for the $AsMe_2$ ^1H resonances in $AsMe_2$-bridged dinuclear systems,[19] there is a noticeable distinction between the μ_3-PMe ^1H signals for open and closed clusters with the resonances for the closed clusters (**1**, **2**, **6**, **7**) in general being about $^1/_2$ ppm upfield from those of the open clusters (**3**, **4**, **5**). (Taking into account that in $CDCl_3$ the resonances are 0.2–0.5 ppm downfield from their position in C_6D_6, only **6a** deviates from this rule.) This effect is 2 orders of magnitude larger and is reversed in the ^{31}P NMR spectra with the resonances of the μ_3-PMe unit in **6a** and **7** being about 200 ppm downfield from that in **5**.

The main objective of the crystal structure determination of **3a** was the confirmation of the open cluster framework. Figure 1 gives the molecular structure, Table VII lists the relevant structural data. **3a** can be considered a member of the large class of $M_2(\mu\text{-}ER_2)$ complexes for which many structure determinations exist.[21] For compounds like **3a** where one of the R units is an organometallic group the number of known crystal structures is much smaller.[3,7]

Scheme I

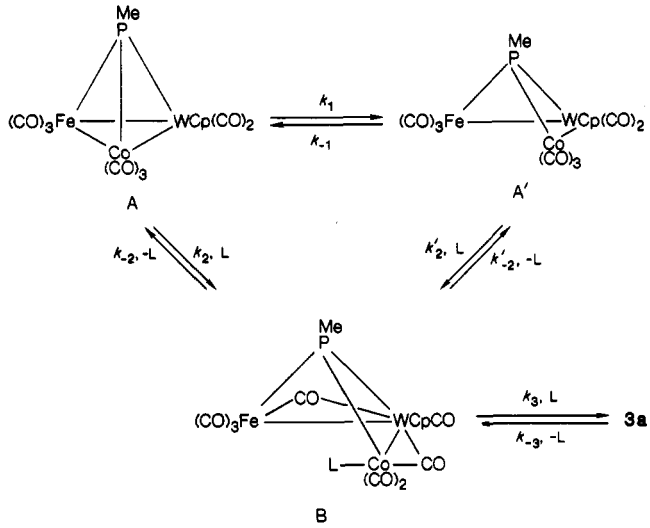

The overall stereochemistry and ligand arrangement in the FePW part of **3a** is quite similar to that in $Cp(CO)_2Mn(\mu\text{-}AsMe_2)Mn(CO)_4$.[22] This includes the slightly bent central CO groups and the length of the metal–metal bond which is long compared to other Fe–W bonds.[23] This sheds light again on the effect of ligand–ligand interactions on metal–metal bond lengths.[21,22] All three metal atoms in **3a** are in typical coordination environments, especially the tbp arrangement around cobalt with both phosphorus ligands in axial positions being in accord with theoretical[24] and experimental[25] observations. It is noticeable, however, that all three bulky ligands (Cp and two PMe_3) point away from the center of the molecule. While the external Fe–P and Co–P bonds are of similar and normal length, the internal Co–P bond is 0.08 Å longer than these and the internal Fe–P bond. This may, in a yet unexplained way, be related to the involvement of iron in metal–metal bonding like in the pair of compounds $[Cp(CO)_2Mo]_2(\mu\text{-}X,\mu\text{-}I)$ where in the absence of a Mo–Mo bond (X = I) the Mo–I distance is 0.09 Å longer than when a Mo–Mo bond is present (X = H).[26] Altogether the molecular geometry of **3a** offers no unusual features.

Kinetics and Mechanism. A kinetic study of the cluster opening reaction was undertaken by using dimethylphenylphosphine as the ligand L. The cluster **2a** reacted with L = PMe_2Ph according to the rate law $d[\mathbf{2a}]/dt = k[\mathbf{2a}][L]$ (details see Table II). Similar reactions of **1** were too rapid to study, even at 16 °C with a tenfold excess of phosphine.

Scheme I lists the possible initial steps in the cluster opening reaction. It is realistic to assume that the iron–cobalt bond breaks first, based on the smaller bond energy of first-row transition-metal bonds,[27] and that the first incoming ligand attacks the cobalt atom, based on the experience from substitutions and additions in cobalt-

(20) Carty, A. J. *Top. Stereochem.*, in press.
(21) Cf. Keller, E.; Vahrenkamp, H. *Z. Naturforsch., B: Anorg. Chem., Org. Chem.* **1978**, *33B*, 537 and references cited therein.
(22) Vahrenkamp, H. *Chem. Ber.* **1974**, *107*, 3867.
(23) Busetto, L.; Jeffery, J. C.; Mills, R. M.; Stone, F. G. A.; Went, M. J.; Woodward, P. *J. Chem. Soc., Dalton Trans.* **1983**, 101.
(24) Rossi, A. R.; Hoffmann, R. *Inorg. Chem.* **1976**, *14*, 365.
(25) (a) Lattmann, M.; Morse, S. A.; Cowley, A. H.; Lasch, J. C.; Norman, N. C. *Inorg. Chem.* **1985**, *24*, 1364. (b) Ahmed, F. R.; Ronstan, J. L. A.; Al-Janabi, M. Y. *Inorg. Chem.* **1985**, *24*, 2526.
(26) Curtis, M. D.; Fotinos, N. A.; Han, K. R.; Butler, W. M. *J. Am. Chem. Soc.* **1983**, *105*, 2686.
(27) Baev, A. K.; Connor, J. A.; El-Saied, N. I.; Skinner, H. A. *J. Organomet. Chem.* **1981**, *213*, 151.

Table VIII. Averaged Rate Constants for the Reaction (μ_3-MeP)FeCoW(C_5H_5)(CO)$_8$ + 2PMe$_2$Ph

T, °C	10^2k,[a] M^{-1} s^{-1}	T, °C	10^2k,[a] M^{-1} s^{-1}
16.0	1.66 ± 0.10	34.6	5.78 ± 0.57
22.0	2.68 ± 0.18	37.7	6.68 ± 0.36
28.0	3.59 ± 0.05		

[a] Error limits are quoted at the 95% confidence level.

containing polynuclear systems.[6,28] Then the question remains whether the reaction occurs via initial metal–metal bond opening (dissociative) or via S_N2-type attack of the phosphine (associative).

Scheme I poses the problem that a dissociative preequilibrium involving A′ cannot be identified from the form of the rate law alone. Only if the magnitude of k'_2 is sufficiently large and that of k'_{-2} sufficiently small or if the concentration of attacking ligand can be made sufficiently large could step A ⇄ A′ affect the rate law. Starting from A (or A′) and assuming a steady-state concentration of B and a very small value of k_{-3} (no intermediates can be observed by spectroscopy during the reaction) give the rate laws

$$\frac{d[\mathbf{2a}]}{dt} = \frac{k_3k_2[A][L]^2}{k_{-2} + k_3[L]} \text{ or } \frac{d[\mathbf{2a}]}{dt} = \frac{k_3k'_2[A'][L]^2}{k'_{-2} + k_3[L]}$$

These laws can be examined in the cases of either the first or second phosphine addition being rate-limiting. If the first addition is rate-limiting, then $k_3 >> k_{-2}$ and the law can be approximated as $k_2[A][L]$ (or $k'_2[A'][L]$). If the second addition is rate-limiting, then $k_{-2} >> k_3$ and the law becomes $(k_3k_2/k_{-2})[A][L]^2$ (or $k_3k'_2/k'_{-2})[A'][L]^2$). Altogether, the possible terms in the experimental rate law are given by

$$\frac{d[\mathbf{2a}]}{dt} = (k_{obsd} + k'_{obsd}[L] + k''_{obsd}[L]^2)[A]$$

The rate behavior of the reaction was determined by using a molar excess of phosphine ranging from 10 to 174 to 16 and 22 °C, and the phosphine concentration was plotted against the observed rate constant. The linearity of the plots and the y intercepts of the plots ($-1.33 \times 10^{-4} \pm 1.35 \times 10^{-4}$ s^{-1} at 16.0 °C, $7.14 \times 10^{-4} \pm 4.03 \times 10^{-4}$ s^{-1} at 34.6 °C) imply that the first-order and third-order components of the possible rate law are zero within experimental error, indicating a bimolecular process, taking into account the simplifications mentioned above.

Table VIII lists the observed rate constants. From the variable-temperature measurements of the PMe$_2$Ph reactions the activation parameters $H^‡ = 10.8 \pm 0.7$ kcal mol^{-1} and $S^‡ = -29 \pm 2.5$ cal mol^{-1} deg^{-1} are calculated. Figure 2 shows the corresponding Eyring plot. The strongly negative activation entropy is consistent with the bimolecular rate law observed. The relatively small activation enthalpy suggests that there is a fair amount of bond making in the transition state.

By varying substituents on the p-phenyl position of the ArPMe$_2$ ligand, the effects of changing the electronic contribution to the nucleophilicity of the phosphine without changing the steric contribution were tested. At 22 °C and a 100-fold excess of the phosphine the rate constants were $k = (1.43 \pm 0.14) \times 10^{-2}$ M^{-1} s^{-1} for L = (p-ClC$_6$H$_4$)PMe$_2$ and $k = (4.07 \pm 0.19) \times 10^{-2}$ M^{-1} s^{-1} for L = (p-MeC$_6$H$_4$)PMe$_2$. This is as expected for a nucleophilic reaction since the para group with the greatest electron-withdrawing power causes the slowest rate of reaction.

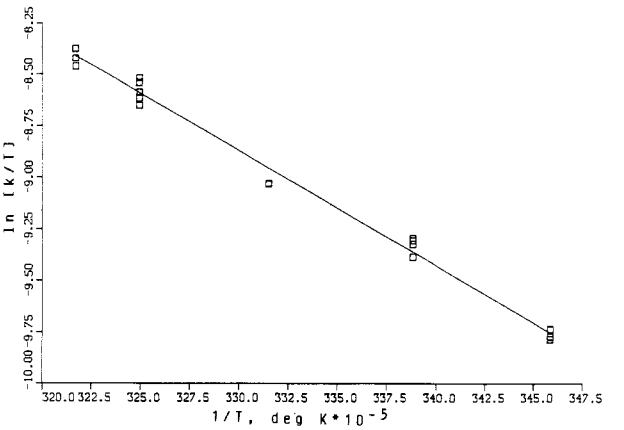

Figure 2. Eyring plot for the reaction of (μ_3-MeP)-FeCoWC$_5$H$_5$(CO)$_8$ with PMe$_2$Ph.

Study of thermal reactions of metal–metal bonded species with donor ligands has often revealed a mixed first- and second-order law, rate = $k_1 + k_2$[L][complex].[29] It has been observed that the k_2 path dominates when L is a good nucleophile, whereas in cases where a first-order mechanism is seen, this mechanism is favored by ligands which are poorer nucleophiles.[7c,29] When these results are compared with the reactions of **2a**, it seems that the corresponding first-order path (k_1 and k_{-1} above) is not available at all, since reaction with PPh$_3$, a poorer nucleophile, only takes place above 60 °C. Thus, even for this phosphine, k_1 and k_{-1} are small, and all kinetic evidence favors an associative mechanism for these cluster openings.

The kinetic behavior of **2a** corresponds to that of (CO)$_4$Fe(μ-AsMe$_2$)Co(CO)$_3$[6b] which also adds phosphine ligands associatively. In contrast to this, the clusters (μ_3-RP)MnFe$_2$Cp(CO)$_8$[7c] just like the dinuclear complex (CO)$_4$Fe(μ-AsMe$_2$)Mn(CO)$_4$[30] show a more complicated kinetic behavior involving dissociative pathways. This may be related to the presence of manganese in the latter complexes but more likely to the fact that the former have a more open and the latter a more crowded ligand sphere. Whereas the clusters (μ_3-RP)MnFe$_2$Cp(CO)$_8$ add two ligands stepwise, there is no indication for intermediates in the addition of two L to **2a**, just as in the case of ligand additions to the clusters (μ_3-RGe)Co$_3$(CO)$_9$.[7b]

As a subsequent reaction, the clean openings of clusters **2** have allowed to study the course of the racemization of clusters **3**. For the one case investigated, this reaction is first order, i.e. intramolecular. It is slow enough to allow an opening–closing sequence, e.g. a ligand substitution, without significant loss of optical purity as was experienced in the enantiomer separation of **2a**.[9] It is also slow enough to allow the isolation of enantiomeric **3b** which is optically stable in the solid state. The open framework of clusters **3** makes it obvious that they racemize easier than the starting clusters with closed tetrahedral frameworks. From our observations that optically active clusters racemize during catalysis runs[8,9] it can therefore be inferred that for these systems the catalytic action involves opening of metal–metal bonds since most substrates of catalysis (CO, olefins, etc.) can act as donor ligands. Mechanistically the

(28) Aime, S.; Milone, L.; Rossetti, R.; Stanghellini, P. L. *Inorg. Chim. Acta* **1977**, *25*, 103.

(29) (a) Candlin, J. P.; Shortland, A. C. *J. Organomet. Chem.* **1969**, *16*, 289. (b) Sonnenberger, D.; Atwood, J. D. *Inorg. Chem.* **1981**, *20*, 3243.

(30) Jackson, R. A.; Poë, A. J.; Langenbach, H. J.; Vahrenkamp, H., unpublished results.

inversion of **3b** ought to be nontrivial since the phosphorus atom in this compound is still four-coordinate. Without having further proof for this, we propose as an inversion pathway a rotation of the Fe–W unit around the FePW three-center bond, thereby formally considering the phosphorus atom as three-coordinate. At the moment there is, however, no obvious way of testing this hypothesis.

Conclusions

The cluster types 1 and 2 extend the series of clusters that can be opened by addition of donor ligands.[3,7,9] They differ from the previously studied μ_3-PR-bridged trimetal systems in that they add two PR_3 ligands showing no noticeable intermediate and that reversal to the closed cluster framework is possible by loss of CO only or by loss of CO and PR_3. For the one case studied kinetically an associative mechanism is indicated for the rate-determining step in complete analogy to dinuclear $FeCo(\mu\text{-}AsMe_2)$ systems. A significant stereochemical information has been obtained in the observation that optical activity is maintained in this type of cluster opening but that the open cluster framework sustains slow inversion. This puts a serious limitation on the transfer of stereochemical information in conversions that may involve cluster framework reactions.

Although the cluster types 1 and 2 demonstrate again that ligand substitution on clusters can occur by an addition–elimination sequence, this will certainly not be the case for all custers. Future investigations should elucidate which factors (besides just metal–metal bond strengths) determine the preference of clusters for "internal" or "external" substitution mechanisms that in turn should offer a better understanding for the still ill-defined area of cluster catalysis.

Acknowledgment. This work was supported by the Deutsche Forschungsgemeinschaft, the Alexander von Humboldt-Stiftung, and the Fonds der Chemischen Industrie. We thank Mr. C. de Meric de Bellefon and Mr. J.-L. Richert, Strasbourg, for ^{31}P NMR measurements, Dr. K. Steinbach, Marburg, for mass spectra, and the Rechenzentrum der Universität Freiburg for computer time.

Supplementary Material Available: Tables containing all distances and angles for **3a** (7 pages); a listing of F_o/F_c for **3a** (13 pages). Ordering information is given on any current masthead page.

Use of Organolithium Reagents in the Synthesis of Diiron Complexes with Bridged and Terminal Carbene Ligands. X-ray Structures of $(CO)_3Fe\{\mu\text{-}C(OEt)\text{-}\eta^2\text{-}C_6H_4NMe_2\}Fe(CO)_3$ and $(CO)_3Fe\{S(CH_2)_3S\}Fe(CO)_2\{C(OEt)Ph\}$

Simon Lotz,*[1] Petrus H. van Rooyen,[2] and Marthie M. van Dyk[1]

Department of Chemistry, University of Pretoria, and the National Chemical Research Laboratory, Council for Scientific and Industrial Research, Pretoria, 0002 South Africa

Received August 21, 1986

Reaction of iron pentacarbonyl with *o*-$MeXC_6H_4Li$ (X = O, NMe), followed by alkylation of the acylmetalate with $[Et_3O]BF_4$, gave the methylene-bridged complexes $(CO)_3Fe\{\mu\text{-}C(OEt)\text{-}\eta^2\text{-}C_6H_4XMe\}Fe(CO)_3$. Substitution of two carbonyls from the complex where X = O with $P(OMe)_3$ yielded $(CO)_2\{P(OMe)_3\}Fe\{\mu\text{-}C(OEt)\text{-}\eta^2\text{-}C_6H_4OMe\}Fe\{P(OMe)_3\}(CO)_2$ as the main product. The complexes $(CO)_3Fe\{S(CH_2)_3S\}Fe(CO)_2\{C(OEt)R\}$ (R = *n*-Bu, Me, Ph), which have terminal carbene ligands, were synthesized from $(CO)_3Fe\{S(CH_2)_3S\}Fe(CO)_3$ and organolithium reagents. The structures of $(CO)_3Fe\{\mu\text{-}C(OEt)\text{-}\eta^2\text{-}C_6H_4NMe_2\}Fe(CO)_3$ (II) and $(CO)_3Fe\{S(CH_2)_3S\}Fe(CO)_2\{C(OEt)Ph\}$ (VII) were confirmed by X-ray crystallography. The crystals of II are monoclinic, space group $P2_1/n$, with a = 9.180 (3) Å, b = 18.636 (4) Å, c = 10.890 (5) Å, β = 95.62 (4)°, and Z = 4. The crystals of VII are monoclinic, space group $P2_1/c$, with a = 8.909 (2) Å, b = 15.028 (3) Å, c = 15.203 (13) Å, β = 102.39 (4)°, and Z = 4. The final R factors are R = 4.7% and R_w = 3.0% for II and R = 9.3% and R_w = 4.8% for VII.

Introduction

Five-coordinate metallacyclic complexes of iron-containing carbene–carbon and hetero donor atoms in five-membered chelate rings are scarce (Chart I). In a reaction of $Fe(CO)_5$ with LiN-*i*-Pr_2 and subsequent treatment with $[Et_3O]BF_4$, the cyclic carbene complex $Fe(CO)_3\{C(N\text{-}i\text{-}Pr_2)OC(O)Et\}$ was found as a minor product in low yield.[3]

Chart I

By contrast, chelates of this kind are well-known for chromium with heteroatoms O, S, N, and P.[4-7] Since

(1) University of Pretoria.
(2) The National Chemical Research Laboratory of the CSIR.
(3) Fischer, E. O.; Schneider, J.; Ackermann, K. *Z. Naturforsch., B: Anorg. Chem., Org. Chem.* **1984**, *39B*, 468.
(4) Dötz, K. H.; Fügen-Koster, B.; Neugebauer, D. *J. Organomet. Chem.* **1979**, *277*, 489.
(5) Raubenheimer, H. G., Lotz, S.; Viljoen, H. W.; Chalmers, A. A. *J. Organomet. Chem.* **1978**, *152*, 73.

0276-7333/87/2306-0499$01.50/0